

See discussions, stats, and author profiles for this publication at: <https://www.researchgate.net/publication/225085154>

# Polyelectrolyte-Surfactant Complex as a Template for the Synthesis of Zeolites with Intracrystalline Mesopores

ARTICLE in LANGMUIR · MAY 2012

Impact Factor: 4.46 · DOI: 10.1021/la300447n · Source: PubMed

---

CITATIONS

13

READS

66

## 7 AUTHORS, INCLUDING:



Jingui Wang

Nanyang Technological University

36 PUBLICATIONS 580 CITATIONS

[SEE PROFILE](#)



Na Li

Chinese Academy of Sciences

212 PUBLICATIONS 5,530 CITATIONS

[SEE PROFILE](#)

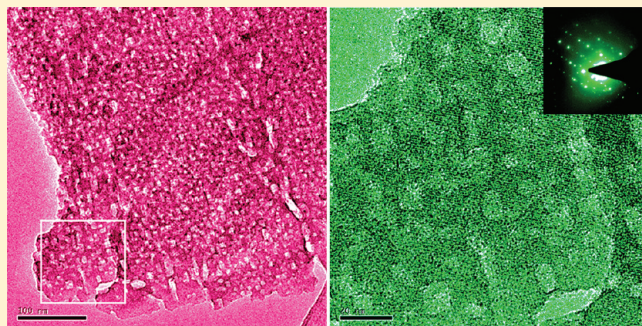
## Polyelectrolyte–Surfactant Complex as a Template for the Synthesis of Zeolites with Intracrystalline Mesopores

Jin-Yu Liu, Jin-Gui Wang, Na Li, Hui Zhao, Hui-Jing Zhou, Ping-Chuan Sun, and Tie-Hong Chen\*

Institute of New Catalytic Materials Science, Key Laboratory of Advanced Energy Materials Chemistry (MOE), College of Chemistry, Nankai University, Tianjin 300071, China

### S Supporting Information

**ABSTRACT:** Mesoporous zeolite silicalite-1 and Al-ZSM-5 with intracrystalline mesopores were synthesized with polyelectrolyte–surfactant complex as the template. Complex colloids were first formed by self-assembly of the anionic polymer poly(acrylic acid) (PAA) and the cationic surfactant cetyltrimethylammonium bromide (CTAB) in basic solution. During the synthesis procedure, upon the addition of the silica source, microporous template (tetrapropylammonium hydroxide), and NaCl, these PAA/CTA complex colloids underwent dissociation and gave rise to the formation of hollow silica spheres with mesoporous shells templated by CTAB micelles and PAA domains as the core. Under hydrothermal treatment, the hollow silica spheres gradually merged together to form larger particles with the PAA domains embedded as the space occupant, which acted as a template for intracrystalline mesopores during the crystallization of the zeolite framework. Amphiphilic organosilane was used to enhance the connection between the PAA domain and the silica phase during the synthesis. After calcination, single crystal-like zeolite particles with intracrystalline mesopores of about 5–20 nm were obtained, as characterized by X-ray diffraction, scanning electron microscopy, transmission electron microscopy, and N<sub>2</sub> adsorption measurements. With the addition of an aluminum source in the synthesis, mesoporous zeolite Al-ZSM-5 with intracrystalline mesopores was also synthesized, and enhanced catalytic property was observed with mesoporous Al-ZSM-5 in acetalization of cyclohexanone with methanol.



### INTRODUCTION

Polyelectrolyte/surfactant complexes are usually formed by ionic self-assembly between polyelectrolyte (ionic polymer) and the oppositely charged surfactant. Antonietti and co-workers precipitated out organic complexes made of poly(styrenesulfonate) and different alkyltrimethylammonium in water, and the complex exhibited highly ordered mesomorphic phases.<sup>1</sup> Ionic self-assembly of polyelectrolyte and oppositely charged surfactants can form highly ordered mesomorphic liquid crystalline phases and is a versatile tool to create supramolecular materials.<sup>2–5</sup> According to the dielectric properties of polyelectrolyte/surfactant complexes, the electrochemical sensing platforms were presented, which was based on the polyelectrolyte/surfactant supramolecular assembly formed by poly(allylamine) and dodecyl sulfate with incorporating carbon nanotubes.<sup>6</sup> Due to the biomedical application of polyelectrolyte, such as drug delivery, Thüemann et al. designed pH-sensitive nanoparticles formed by poly(amino acid) and dodecanoic acid as relatively simple containers suitable for the incorporation of hydrophobic drugs.<sup>7</sup>

Although organic polyelectrolyte/surfactant complexes were extensively studied, they were rarely utilized to control the mesostructure and morphology of inorganic materials. Recently, Yang et al. reported the synthesis of mesoporous

silica film using polyethylenimine and cationic surfactant complexes as templates.<sup>8</sup> In our previous work,<sup>9</sup> we have reported the synthesis of hierarchically nanoporous single-crystal mesoporous silica SBA-1 by using mesomorphic polyelectrolyte–surfactant complexes as the dynamic template, and the sample possessed the characters of both crystal-like regularity and high diffusion efficiency of hierarchical pores.

Zeolites are microporous crystalline materials with molecular sieve and shape-selective properties, and have been widely used in catalytic, adsorption, and ion exchange processes.<sup>10,11</sup> However, the development of zeolites is restricted in industrial applications on large molecules due to its small size of micropores. To overcome this problem, MCM-41 and SBA-15, as typical representatives of mesoporous materials, were synthesized, which had ordered mesopores and large surface areas.<sup>12,13</sup> Unfortunately, these materials exhibited insufficient hydrothermal stability and weak acidity compared with crystalline zeolites. In recent years, much attention has been focused on the synthesis of mesoporous zeolites, which combine the advantages of zeolites (strong acidity and stability)

Received: January 31, 2012

Revised: May 10, 2012

and mesoporous materials (larger pore and hierarchical structure).<sup>14</sup> Several strategies to fabricate mesopores in zeolite crystals have been reported. Post-treatments destroy the zeolite framework to produce mesopores under acidic or basic conditions. However, this method tends to produce zeolite fragments rather than intracrystalline mesopores during the process of the dealumination or desilication.<sup>15,16</sup> Hard templates, such as carbon nanoparticals,<sup>17</sup> nanotubes,<sup>18</sup> and nanosized  $\text{CaCO}_3$ ,<sup>19</sup> have been employed to produce pores within a zeolite framework; however, the homogeneous dispersion of the nanosized hard templates inside the zeolite synthesis gel was generally hindered due to their interface incompatibility.

Supramolecular templating is a valid method to create intercrystalline or intracrystalline meso-/macroporous zeolite. To solve the phase-separation of the organic template and zeolite framework, Ryoo et al. synthesized a mesoporous zeolite composed of nanocrystals with tunable mesoporosity by amphiphilic organosilanes.<sup>20</sup> By using a specially designed gemini-type, polyquaternary ammonium surfactants, mesoporous molecular sieves with microporous crystalline aluminosilicate pore walls were synthesized.<sup>21</sup> Pinnavaia et al. synthesized a silylated polyethylenimine polymer, which was used as the template for the formation of intracrystal mesopores in zeolite.<sup>22</sup> Xiao et al. synthesized hierarchical mesoporous zeolites templated with a mixture of small organic ammonium salts and cationic polymers.<sup>23</sup> By using a designed cationic amphiphilic copolymer as a template, zeolite ZSM-5 with oriented mesoporous channels was synthesized.<sup>24</sup> Conventional block copolymers were also used as templates to synthesize mesoporous zeolites, and this route should be assisted by a poststeaming treatment to avoid the phase separation between the template and the silica phase.<sup>25</sup>

Generally, cationic polymers were used as scaffolds embedded in the synthesis gel of zeolites to interact with the silica species, which possess negative charges under the alkaline conditions for zeolite crystallization.<sup>22–24</sup> Herein, we report a direct synthesis route to obtain a mesoporous zeolite with extensive intracrystalline mesopores with size of about 5–20 nm, by using polyelectrolyte–surfactant complexes as the template. With this method, via complex formation with the cationic surfactant cetyltrimethylammonium bromide (CTAB), the anionic polymer poly(acrylic acid) (PAA) was introduced into the zeolite precursor framework as a space occupant for intracrystalline mesopores.

## EXPERIMENTAL SECTION

**Chemicals.** CTAB was from Amresco. PAA (average molecular weight 240 000, 25 wt % solution in water) was from Acros Organics. Tetraethyl orthosilicate (TEOS) was purchased from Aladdin, China. [3-(trimethoxysilyl)propyl] octadecyldimethyl ammonium chloride ( $[(\text{CH}_3\text{O})_3\text{SiC}_2\text{H}_6\text{N}(\text{CH}_3)_2\text{C}_{18}\text{H}_{37}]^+$ Cl, abbreviated TPOAc) was from Robiot Co., Ltd., China. Other reagents including tetrapropylammonium hydroxide (TPAOH, 25 wt %), NaOH, NaCl, and  $\text{NH}_3\cdot\text{H}_2\text{O}$  (25 wt %) were purchased from Guangfu Chemical Reagent Company (China). Commercial HZSM-5 zeolite with Si/Al = 23 was from the Tianjin Shen-neng company.

**Preparation of Polyelectrolyte–Surfactant Complexes.** In a typical synthesis, 0.55 g of CTAB was completely dissolved in 25.0 mL of deionized water under stirring, and 3.0 g of PAA (25 wt % solution) was added under vigorous stirring at room temperature to obtain a clear solution. Then drops of ammonia (25%) were gradually added to the clear solution under stirring, and white precipitate appeared to form a gel-like block. If more ammonia was added continuously, the

block gradually disassociated, and after a total of 1.6 g of ammonia was added, the solution (pH was 10.3) became a milky suspension due to the formation of PAA/CTAB complex colloids. The solution was further stirred for 20 min.

**Synthesis of Mesoporous Zeolites.** Mesoporous silicalite-1 was synthesized as follows: 1.8 g of NaCl was dissolved in 5 mL of  $\text{H}_2\text{O}$ , and then 21 g of TPAOH (25 wt %) was added into the above solution under vigorous stir to obtain a clear solution. The as-prepared PAA/CTAB complex suspensions (containing 1.1 g of CTAB and 6.0 g of PAA) were impregnated into the clear solution. After stirring for 20 min, a mixture of 15 g of TEOS and 0.6 g of TPOAc (50% methanol solution) was added under vigorous stirring. The molar composition of the mixture was  $10\text{SiO}_2\cdot3.6\text{TPAOH}\cdot0.08\text{TPOAc}\cdot360\text{H}_2\text{O}\cdot4.2\text{NaCl}$ . The final mixture was further stirred for 2 h at room temperature and was then transferred into an autoclave for further hydrothermal treatment at 140 °C for 6 days. The final product was filtered, washed with deionized water, dried overnight at 80 °C, and finally calcined at 550 °C in air for 6 h. Mesoporous Al-ZSM-5 was also synthesized in a similar way with  $\text{NaAlO}_2$  as the aluminum source and a  $\text{SiO}_2\cdot\text{Al}_2\text{O}_3$  ratio of 100:1.

**Characterization.** Small-angle X-ray scattering (SAXS) experiments were performed on a Bruker Nanostar SAXS system. X-ray diffraction (XRD) patterns were obtained on a Rigaku D/max-2500 diffractometer, with  $\text{CuK}\alpha$  Radiation at 40 kV and 100 mA. The XRD patterns were collected in the range of 5–50° in  $2\theta/\theta$  scanning mode with a 0.02° step and scanning speed of 12 degree/min. Transmission electron microscopy (TEM) observations were performed on a Philips Tecnai F20 microscope, working at 200 kV. All samples subjected to TEM measurements were dispersed in methanol ultrasonically and were dropped on copper grids. Scanning electron microscopy (SEM) images were obtained with a Shimadzu SS-550 and a Hitachi S-4800 instrument. Nitrogen adsorption and desorption isotherms were measured on a BELSORP-mini II sorption analyzer at 77 K. Specific surface area was calculated by the BET (Brunauer–Emmett–Teller) method based on the adsorption data at  $P/P_0$  of 0.05–0.2. The pore-size distribution was calculated from the adsorption branch using the BJH (Barrett–Joyner–Halenda) method, and total pore volume was obtained from the adsorption at  $P/P_0 = 0.95$ . Micropore volume was calculated by a *t*-plot curve. Elemental analysis for the Si/Al ratio was performed with inductively coupled plasma atomic emission spectroscopy (ICP-AES) using a Thermo Jarrell-Ash ICP-9000(N+M)).

**Catalytic Reaction.** The mesoporous Al-ZSM-5 was ion exchanged in 1.0 M  $\text{NH}_4\text{NO}_3$  solution at 100 °C for 2 h, and the process was repeated three times. The  $\text{NH}_4^+$  form zeolite was calcined at 550 °C for 2 h to obtain  $\text{H}^+$  form Al-ZSM-5. The acetalization of cyclohexanone was carried out in a round-bottomed flask equipped with a reflux condenser. In the typical reaction, 0.2 g of cyclohexanone and 25 mg Al-ZSM-5 was diluted with 5 mL methanol. The reaction was performed at 50 °C for 1 h under atmospheric pressure. The liquid supernatant was analyzed by a gas chromatograph (GC-7800) with a flame ionization detector, using a FFAP and  $\text{N}_2$  as carrier gas. The conversion was calculated based on cyclohexanone.

## RESULTS AND DISCUSSION

The XRD pattern of the mesoporous silicalite-1 synthesized at 140 °C for 6 d is shown in Figure 1a. The sample exhibited the characteristic diffraction peaks at  $2\theta$  of 7.9°, 8.8°, 23.1°, 23.7°, 23.9° and 24.4°, respectively, which were indexed to the structure of mordenite framework inverted (MFI) topology.<sup>26</sup> The SEM images showed that the particle size of the mesoporous silicalite-1 was in the range of 20–30  $\mu\text{m}$ , and the surface of the particle was composed of needle-like crystal fibers (Figure 2). Typical TEM images of the mesoporous silicalite-1 are shown in Figure 3, and well-dispersed intracrystal mesopores could be clearly observed. In the high-resolution TEM images (Figure 3b,d) well-ordered crystal lattice fringes are clearly shown, indicating high crystallinity of the product. The electron diffraction patterns (insets in Figure 3b,d)

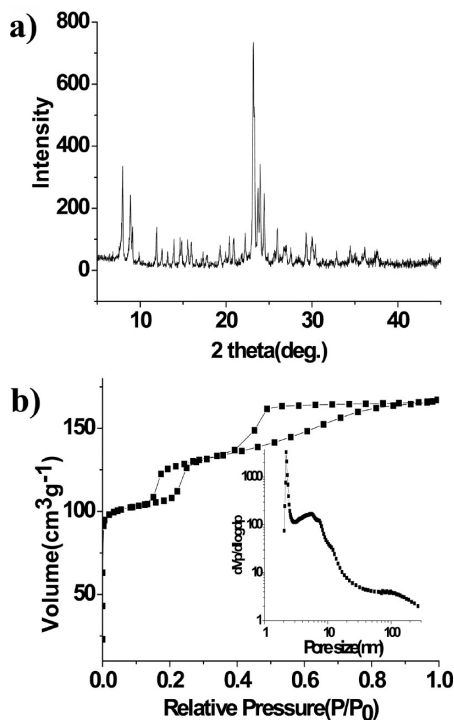


**Figure 1.** (a) XRD pattern and (b) nitrogen adsorption–desorption isotherms and BJH pore size distribution (inset) of the calcined mesoporous silicalite-1 synthesized at 140 °C for 6 days.

indicate that the mesoporous silicalite-1 remained a single crystal even with intracrystalline mesopores. The pore size of the intracrystalline mesopores was mainly in the range of 5–20 nm, and this was also proved by nitrogen adsorption discussed below. Although amphiphilic organosilane TPOAc was used in our synthesis, the mesoporous silicalite-1 exhibited single crystal-like structure with embedded intracrystalline mesopores, and this structure characteristic is different from the mesoporous zeolites in other reports synthesized with the aid of organosilane, in which mesoporous zeolite particles were mainly built with zeolite nanocrystals randomly aggregated or stacked with some degree of orientation.<sup>20,27–29</sup>

The nitrogen adsorption isotherms (Figure 1b) of the mesoporous silicalite-1 exhibited two distinct adsorption steps at relative pressures  $P/P_0$  of 0.15–0.25 and  $P/P_0$  of 0.4–0.9. As reported by previous work,<sup>30</sup> the hysteresis loop at about  $P/P_0$  of 0.2 could be explained by a fluid-to-crystal-like phase transition of nitrogen molecules in the micropores. For this reason, although in the pore size distribution curve the step at

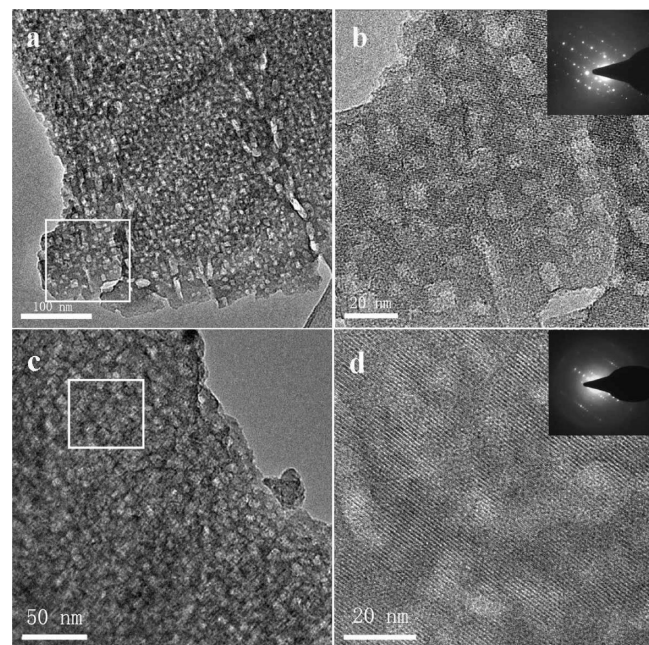


**Figure 3.** TEM images of mesoporous silicalite-1. The insets in panels b and d are the corresponding electron diffraction patterns.

$P/P_0 \approx 0.2$  gave rise to a sharp peak at about 2.2 nm, it could not be considered as real porosity. The second adsorption step exhibited a large hysteresis loop at relative pressure  $P/P_0$  of 0.4–0.9, which was attributed to the capillary condensation of nitrogen in the mesopores. This adsorption step gave rise to a broad pore size distribution range of about 5–20 nm (Figure 1b, inset), indicating the hierarchically porous structure of the mesoporous silicalite-1.

Combining the results of XRD, N<sub>2</sub> adsorption, SEM and TEM characterizations, it can be concluded that mesoporous silicalite-1 crystals with embedded intracrystalline mesopores were successfully synthesized. To understand the formation mechanism of the intracrystalline mesopores, the synthesis process was monitored at different steps. In our synthesis, when anionic polymer PAA and cationic surfactant CTAB were dissolved in water, a clear solution was obtained. With the gradual addition of ammonia, the solution was tuned to basic, and the carboxylic acid groups were neutralized to carboxyl anions, which would interact with the cationic surfactant CTAB and lead to the formation of white PAA–CTA complex precipitate. The hydrogen bonds between hydroxyls and carboxyl oxygen from different PAA chains would also contribute to the macro block of the complexes. As shown in

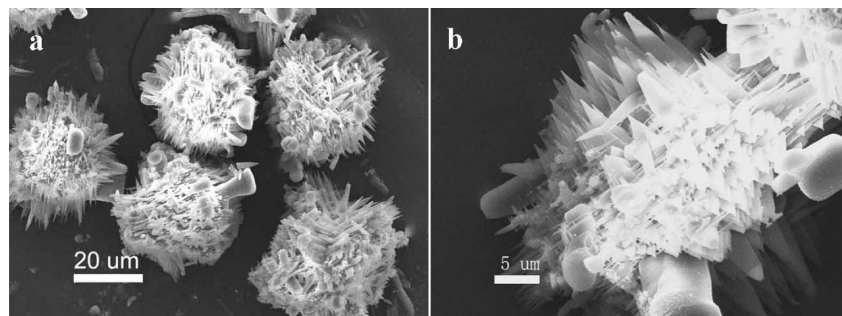


**Figure 2.** SEM images of mesoporous silicalite-1 synthesized at 140 °C for 6 days.

Figure 4a,b, the precipitated complex looked like chewing gum, and it could be easily stretched. The SAXS pattern of the bock

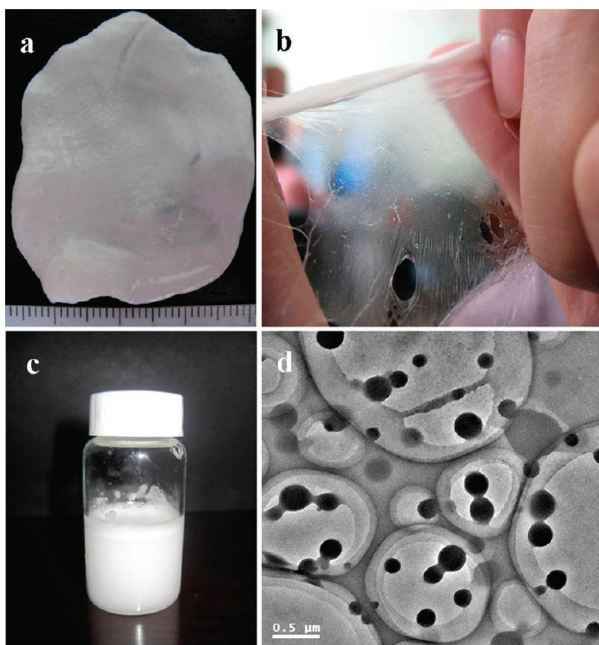


**Figure 4.** The pictures of PAA–CTA complexes: (a) A white soft solid. (b) Transparent thin film was obtained by extending. (c) The milky PAA–CTA complexes solution. (d) TEM image of the milky PAA–CTA complexes.

complex displayed three diffraction peaks as shown in Figure S1a (Supporting Information), indicating an ordered cubic  $Pm\bar{3}n$  mesostructure. With more ammonia addition, some hydrogen bonds between PAA chains were disturbed, and the block precipitate gradually disassociated to form complex colloids, and the solution was eventually turned into a milky emulsion (Figure 4c). If the emulsion was dropped on a copper grid for TEM observation, the image showed that dispersed submicrometer organic complex particles were formed (Figure 4d). SAXS pattern of the PAA–CTA complex colloids obtained by centrifugation showed three distinct diffraction peaks indexed to (200), (210), and (211) diffraction peaks, respectively, indicating that they also exhibited a highly ordered cubic  $Pm\bar{3}n$  mesostructure (Figure S1b).

Upon the addition of the other reactants, including TPAOH, NaCl, TEOS, and TPOAc, to the PAA–CTA complex suspension, the mixture was stirred for 2 h, and a white suspension was obtained. TEM observation was performed with the drops of the suspension on a copper grid, and it was interesting to find that the product at this moment was composed of hollow spheres with wormhole-like mesoporous shells (Figure 5a,b). The size of the hollow spheres was about several hundreds of nanometers, and these hollow spheres tended to aggregate together; some of them had even already fused together. Obviously, the less-ordered, wormhole-like mesopores in the shell were templated by the CTA micelles, and this indicates that the well-ordered  $Pm\bar{3}n$  mesostructure of the PAA–CTA complex collapsed after the addition of other reactants. In other studies of polyelectrolyte/surfactant complexes, it has been shown that the addition of salts reduces the strength of electrostatic interaction between surfactants and polyelectrolytes, and could even completely screen the

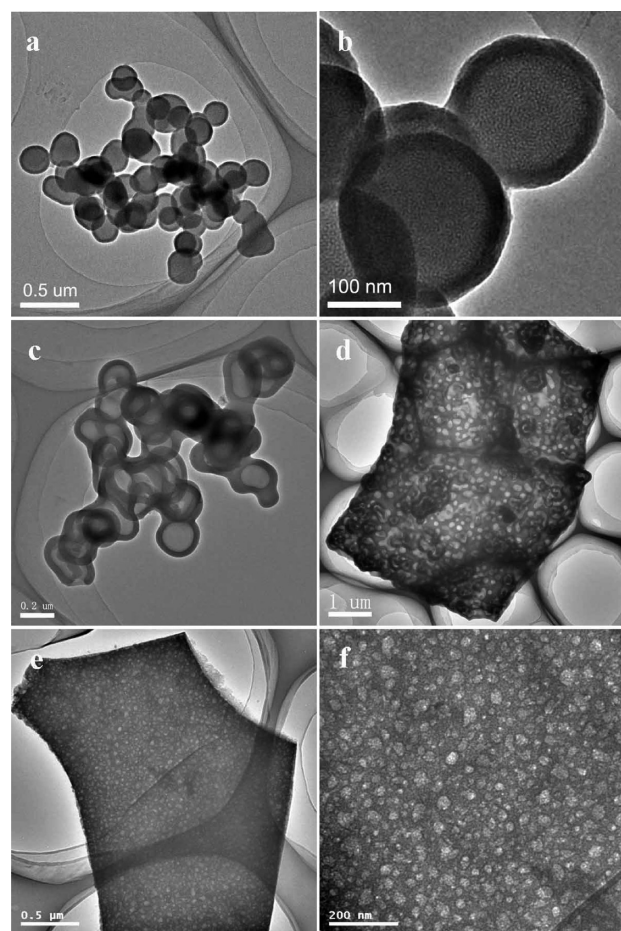


**Figure 5.** TEM image of the intermediate products in the formation process of mesoporous silicalite-1: (a,b) drops of the mixed reactants solution after stirring for 2 h; (c,d) product after reaction at 80 °C for 2 days; (e,f) product after reaction at 120 °C for 6 days.

electrostatic interaction and result in partial or complete dissociation of the polyelectrolyte/surfactant complexes.<sup>31–33</sup> Here in our case, the  $\text{Na}^+$  and  $\text{TPA}^+$  competed with the CTA surfactant to interact with PAA, and this considerably decreased the amount of surfactants bound to the polyelectrolyte and resulted in dissociation of the mesostructured PAA/CTA complexes. Then the ordered PAA/CTA complexes dissociated and evolved to CTA-coated PAA complexes. The dissociated CTA micelles coassembled with the silica precursors and formed a wormhole-like mesostructured shell, with the phase-separated PAA domains as the core, thus giving rise to the hollow spheres. The fusion of the hollow spheres was either due to the aggregation of the CTA-coated PAA complex colloids, due to cross-linking of the silica, or due to both of these effects. The presence of both PAA and CTAB is essential to the formation of hollow spheres, because if CTAB was not added in the synthesis, after mixture of the reactants and 2 h of stirring, only irregular solid and nonporous particles were observed by TEM (Figure S2a). If PAA was not added, only particles with wormhole-like mesopores were observed by TEM measurements (Figure S2b).

Although in our work the mesoporous zeolite was synthesized at 140 °C for 6 d, for a better observation of the intermediate products during the synthesis process, the synthesis was also performed at different temperatures for different times. After reaction at 80 °C for 2 d, the product was

collected and calcined for different characterizations. TEM images of the product indicated that severely merged hollow silica spheres formed patches with extensively embedded voids (Figure 5c,d). The XRD pattern indicated that there still existed less-ordered mesostructure but without the crystallinity of a zeolite (Figure 6a), and the N<sub>2</sub> adsorption data also showed the

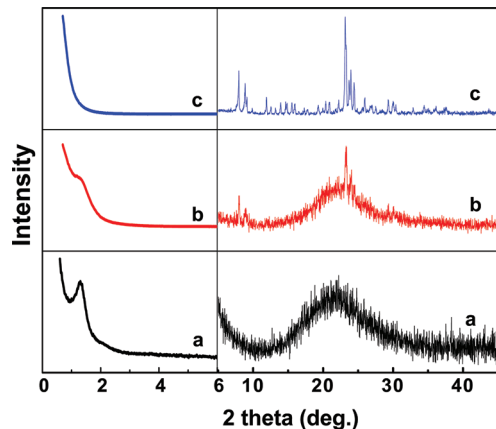


**Figure 6.** XRD patterns of (a) product after reaction at 80 °C for 2 days, (b) product after reaction at 120 °C for 6 days, and (c) mesoporous silicalite-1 synthesized at 140 °C for 6 days.

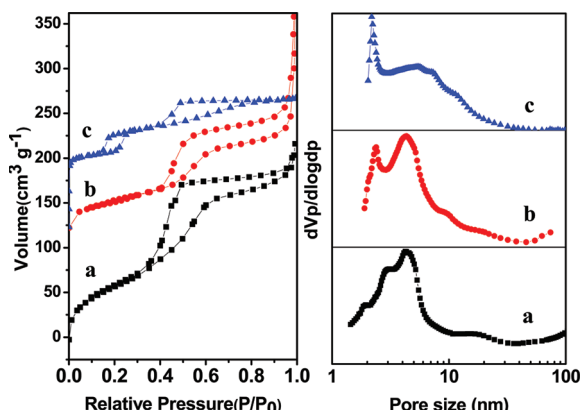


**Figure 7.** Nitrogen adsorption–desorption isotherms and pore size distribution curves of (a) product after reaction at 80 °C for 2 days, (b) product after reaction at 120 °C for 6 days, and (c) mesoporous silicalite-1 synthesized at 140 °C for 6 days.

mesoporous structure of the silica wall (Figure 7a, and the porosity parameters are listed in Table 1). If the synthesis was performed at 120 °C for 6 days, TEM images of the calcined product showed the voids had greatly shrank to the size of about 20–50 nm due to the further condensation of the silica wall during the continuous hydrothermal treatment (Figure 5e,f). The XRD pattern indicated that the mesoscale order almost disappeared because the mesostructured silica templated by CTAB micelles was gradually collapsed by the hydrothermal treatment at 120 °C for 6 days (Figure 6b), as was also proved by the N<sub>2</sub> adsorption measurement (Figure 7b and Table 1). Meanwhile, traces of diffraction peaks of the MFI zeolite structure began to emerge. As the temperature increased to 140 °C for 6 days, the silica wall was transformed into a zeolite crystal phase templated by TPA, while the embedded

**Table 1. Texture Parameters of Mesoporous Zeolites and Intermediate Products**

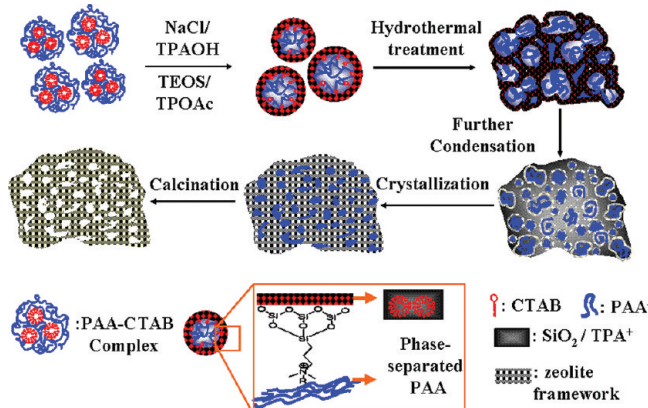
sample	$S_{\text{BET}}^a$ ( $\text{m}^2 \cdot \text{g}^{-1}$ )	$V_{\text{total}}^b$ ( $\text{cm}^3 \cdot \text{g}^{-1}$ )	$V_{\text{micro}}^c$ ( $\text{cm}^3 \cdot \text{g}^{-1}$ )	$V_{\text{meso}}^d$ ( $\text{cm}^3 \cdot \text{g}^{-1}$ )
MS-80 <sup>d</sup>	297	0.33		0.33
MS-120 <sup>e</sup>	180	0.23	0.06	0.17
mesoporous silicalite-1	420	0.26	0.15	0.11
mesoporous Al-ZSM-5	350	0.25	0.14	0.11
MS-No TPOAc <sup>f</sup>	360	0.19	0.16	0.03

<sup>a</sup> $S_{\text{BET}}$ , surface area obtained from N<sub>2</sub> adsorption isotherms. <sup>b</sup> $V_{\text{total}}$ , total pore volume obtained at  $P/P_0 = 0.95$ . <sup>c</sup> $V_{\text{micro}}$ , micropore volume is calculated from the *t*-plot method. <sup>d</sup>Product obtained after reaction at 80 °C for 2 days. <sup>e</sup>Product obtained after reaction at 120 °C for 6 days. <sup>f</sup>Product synthesized at 140 °C for 6 days but without the addition of TPOAc.

mesopores further shrank to give rise to the intracrystalline mesopores of 5–20 nm (as shown in Figure 3).

On the basis of the above results, a tentative mechanism was proposed to illustrate the formation mechanism of mesoporous silicalite-1. As shown in Scheme 1, the ordered PAA-CTAB

**Scheme 1. Schematic Illustration of the Formation Mechanism of Mesoporous Silicalite-1**



complexes were first formed under alkaline conditions. While the reactants of TPAOH, NaCl, TEOS, and TPOAc (amphiphilic organosilanes) were added to the PAA–CTAB complex suspension, the addition of cations ( $\text{Na}^+$  and  $\text{TPA}^+$ ) competed with surfactant to interact with PAA, considerably decreasing the amount of surfactant bound to the polyelectrolyte. The ordered PAA/CTA complex underwent dissociation and evolved to a CTA-coated PAA complex, then the negatively charged inorganic silica ions/oligomers produced by the hydrolysis of TEOS could interact with cationic CTA micelles; thus silica hollow spheres were formed with CTA-templated mesostructured silica as the shell and the phase-separated PAA domains as the core. During further hydrothermal treatment, fusion of the hollow spheres occurred either due to the aggregation of the CTA-coated PAA complex colloids, due to the cross-link of the silica, or due to both of these effects. Meanwhile, the mesostructured silica templated by CTA micelles gradually collapsed due to the increasing temperature, and the voids templated by PAA domains gradually shrank because the condensation of the silica wall gradually expelled some of the PAA chains into the solution.

With the further crystallization of the silica wall templated by TPA cations, more PAA chains were expelled, and the voids occupied by PAA domains continuously shrank, giving rise to intracrystalline mesopores with size of about 5–20 nm. After calcination, both the micropore template TPA cations and embedded remaining mesopore template PAA chains were burned out, and mesoporous silicalite-1 crystals were obtained.

Amphiphilic TPOAc organosilanes played an important role in the connection between the silica wall and the phase-separated PAA domains. The hydrolyzable methoxysilyl moiety could form covalent bonds with  $\text{SiO}_2$  sources, and the positively charged alkylammonium moiety could strongly interact with the negatively charged PAA. To further demonstrate the role of TPOAc, we also synthesized silicalite-1 without the addition of TPOAc. SEM images reveal that the silicalite-1 synthesized without TPOAc exhibited uniform morphology (Figure 8a,b).

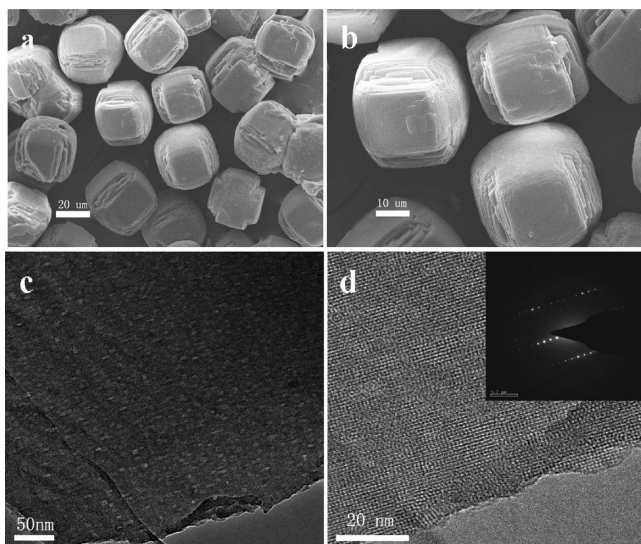


**Figure 8.** SEM (a,b) and TEM (c,d) images of silicalite-1 synthesized without the addition of amphiphilic organosilane TPOAc.

TEM images (Figure 8c) show a few mesopores with the size of about 2–5 nm. Uniform crystallographic orientation lattice was shown in the high-resolution TEM image, indicating that the sample was a single crystal (Figure 8d). The nitrogen adsorption–desorption isotherms indicate that a small hysteresis loop at  $0.4 < P/P_0 < 0.8$  due to the deficient mesopores (Figure 9). Adsorption parameters also indicate that the mesopore volume decreased from  $0.11 \text{ cm}^3 \cdot \text{g}^{-1}$  of mesoporous silicalite-1 to  $0.03 \text{ cm}^3 \cdot \text{g}^{-1}$  (see Table 1).

In order to enhance the acidic sites for catalytic reaction, by adding aluminum source in our synthesis, mesoporous Al-ZSM-5 was also synthesized. As shown in Figure 10a, the morphology of the mesoporous Al-ZSM-5 was tuned to irregular spheres. TEM images show similar intracrystalline mesopores as mesoporous silicalite-1, and the corresponding high-resolution TEM images also display single-crystalline zeolite phases with embedded mesopores (Figure 10b–d). The XRD pattern indicates well-crystallized ZSM-5 structure (Figure 11a), and the nitrogen adsorption isotherm (Figure 11b) was similar to that of the mesoporous silicalite-1. The  $^{27}\text{Al}$  magic angle spinning (MAS) NMR spectra of mesoporous Al-ZSM-5 before and after calcination show signal at about 55 ppm (Figure 12), which was assigned to tetrahedrally coordinated aluminum. The catalytic activity of the mesoporous

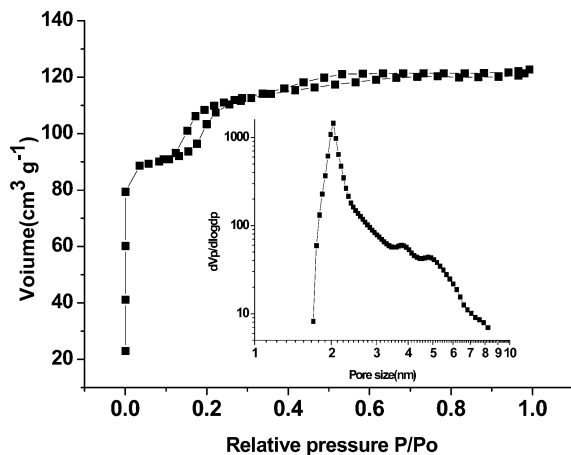


**Figure 9.** Nitrogen adsorption–desorption isotherms and BJH pore size distribution of silicalite-1 synthesized without the addition of amphiphilic organosilane TPOAc.

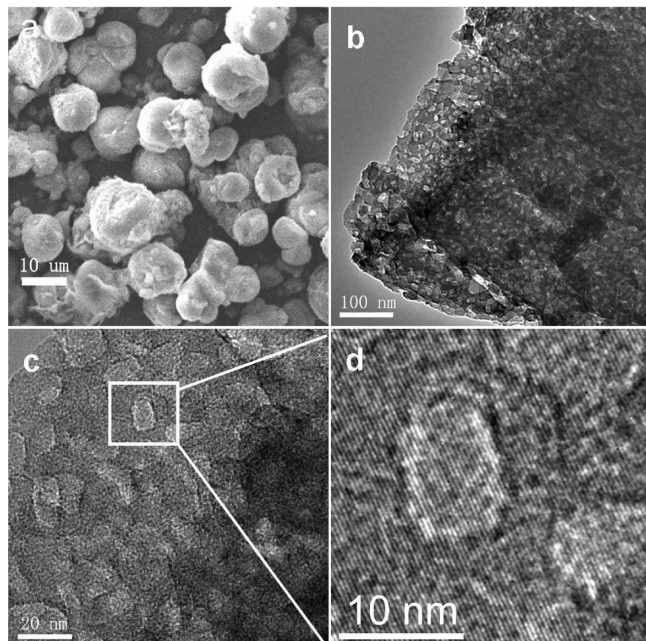


**Figure 10.** (a) SEM and (b–d) TEM images of the calcined mesoporous Al-ZSM-5.

Al-ZSM-5 was tested by acetalization of cyclohexanone with methanol, and the result was compared with that of the commercial HZSM-5 ( $\text{Si}/\text{Al} = 23$ ). As shown in Table 2, for mesoporous Al-ZSM-5 ( $\text{Si}/\text{Al}=55$ ), the conversion of the cyclohexanone at 1 h was higher than that of the commercial HZSM-5, even though the Al content in the mesoporous Al-ZSM-5 was only around half that of the commercial HZSM-5. This indicates that the enhanced diffusion of the organic species within the mesoporous zeolite crystals is a benefit to the catalytic reaction.

Although it has been demonstrated that with the PAA/CTA complex as a template, zeolites with intracrystalline mesopores could be prepared, further work is still necessary, including adjustment of the ratios of the reactants, selection of different anionic polymers, cationic surfactants, micropore templates, and so forth. Concerning the low cost and diverse types of the anionic polymers and cationic surfactants, as well as the

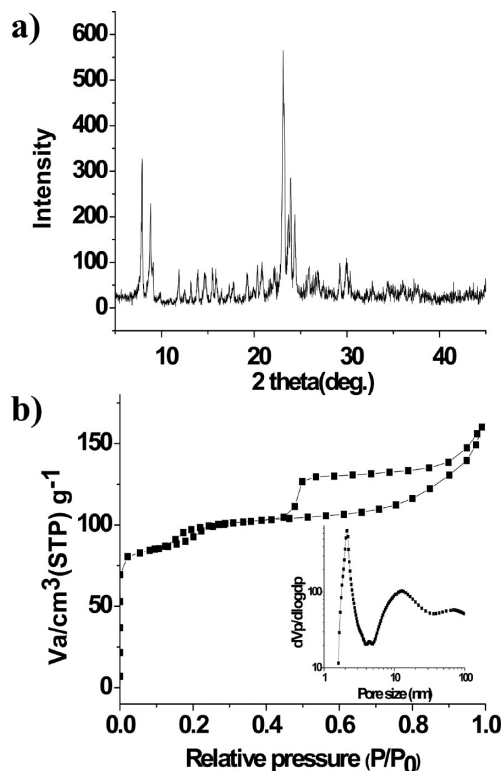


**Figure 11.** (a) XRD pattern and (b) nitrogen adsorption–desorption isotherms and BJH pore size distribution of the calcined mesoporous Al-ZSM-5.

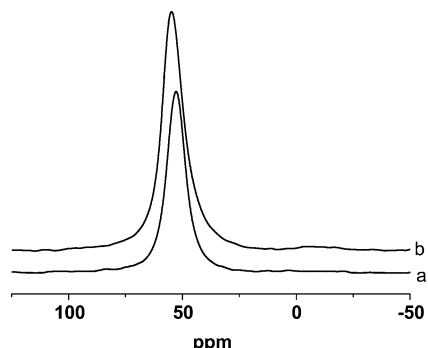


**Figure 12.**  $^{27}\text{Al}$  MAS NMR of (a) the as-synthesized and (b) calcined mesoporous Al-ZSM-5.

commercial availability of the organosilane TPOAc, the synthesis method reported here could be well expanded for the synthesis of other zeolites, such as Beta and Y, with

**Table 2. Catalytic Activity of Mesoporous Al-ZSM-5<sup>a</sup>**

catalyst	Si/Al <sup>b</sup>	conversion (%)
mesoporous Al-ZSM-5	55	85%
commercial HZSM-5	23	76%

<sup>a</sup>The selectivity to 1,1-dimethoxycyclohexane is 100%. <sup>b</sup>The Si/Al mole ratios measured by ICP-AES analysis.

enhanced mesoporous textual structures and improved catalytic properties.

## CONCLUSION

Mesoporous silicalite-1 and Al-ZSM-5 with intracrystalline mesopores were synthesized with polyelectrolyte–surfactant complexes as the template. Complex colloids were first formed by self-assembly of anionic polymer PAA and cationic surfactant CTAB. During the synthesis procedure, upon the addition of the silica source, microporous template (TPAOH), and sodium cations, these PAA/CTA complex colloids underwent dissociation and gave rise to the formation of hollow silica spheres with mesoporous shells templated by CTAB micelles and PAA domains as the core. Under hydrothermal treatment, the hollow silica spheres gradually merged together to form larger particles with the PAA domains imbedded as the space occupant, which acted as a template for intracrystalline mesopores during the crystallization of the zeolite framework. Amphiphilic organosilane enhanced the connection between the PAA domain and silica phase during the synthesis. After calcination, single crystal-like zeolite particles with intracrystalline mesopores of about 5–20 nm were obtained. With the addition of an aluminum source in the synthesis, zeolite Al-ZSM-5 with intracrystalline mesopores was also synthesized, and enhanced catalytic property was observed for the mesoporous Al-ZSM-5 in acetalization of cyclohexanone with methanol.

## ASSOCIATED CONTENT

### Supporting Information

SAXS patterns and TEM images. This information is available free of charge via the Internet at <http://pubs.acs.org/>.

## AUTHOR INFORMATION

### Corresponding Author

\*E-mail address: chenth@nankai.edu.cn.

### Notes

The authors declare no competing financial interest.

## ACKNOWLEDGMENTS

This work was supported by the National Science Foundation of China (Grants 20873070 and 20973095), the National Basic Research Program of China (2009CB623502), and the NCET of Ministry of Education (NCET-07-0448) and MOE (IRT-0927).

## REFERENCES

- (1) Antonietti, M.; Conrad, J.; Thünemann, A. Polyelectrolyte–Surfactant Complexes: A New Type of Solid, Mesomorphic Material. *Macromolecules* **1994**, *27*, 6007–6011.
- (2) Faul, C. F. J.; Antonietti, M. Ionic Self-Assembly: Facile Synthesis of Supramolecular Materials. *Adv. Mater.* **2003**, *15*, 673–683.
- (3) Kogej, K. Association and Structure Formation in Oppositely Charged Polyelectrolyte–Surfactant Mixtures. *Adv. Colloid Interface Sci.* **2010**, *158*, 68–83.
- (4) Zhou, S.; Chu, B. Assembled Materials: Polyelectrolyte Surfactant Complexes. *Adv. Mater.* **2000**, *12*, 545–556.
- (5) Sokolov, E. L.; Yeh, F.; Khokhlov, A.; Chu, B. Nanoscale Supramolecular Ordering in Gel–Surfactant Complexes: Sodium Alkyl Sulfates in Poly(diallyldimethylammonium chloride). *Langmuir* **1996**, *12*, 6229–6234.
- (6) Cortez, M. L.; Ceolin, M.; Azzaroni, O.; Battaglini, F. Electrochemical Sensing Platform Based on Polyelectrolyte-Surfactant

- Supramolecular Assemblies Incorporating Carbon Nanotubes. *Anal. Chem.* **2011**, *83*, 8011–8018.
- (7) General, S.; Thünemann, A. F. pH-Sensitive Nanoparticles of Poly(amino acid) Dodecanoate Complexes. *Int. J. Pharm.* **2001**, *230*, 11–24.
- (8) Yang, B.; Edler, K. J. Free-Standing Ordered Mesoporous Silica Films Synthesized with Surfactant–Polyelectrolyte Complexes at the Air/Water Interface. *Chem. Mater.* **2009**, *21*, 1221–1231.
- (9) Wang, J. G.; Zhou, H. J.; Sun, P. C.; Ding, D. T.; Chen, T. H. Hollow Carved Single-Crystal Mesoporous Silica Templatized by Mesomorphic Polyelectrolyte–Surfactant Complexes. *Chem. Mater.* **2010**, *22*, 3829–3831.
- (10) Corma, A. From Microporous to Mesoporous Molecular Sieve Materials and Their Use in Catalysis. *Chem. Rev.* **1997**, *97*, 2373–2419.
- (11) Corma, A. State of the Art and Future Challenges of Zeolites As Catalysts. *J. Catal.* **2003**, *216*, 298–312.
- (12) Kresge, C. T.; Leonowicz, M. E.; Roth, W. J.; Vartuli, J. C.; Beck, J. S. Ordered Mesoporous Molecular Sieves Synthesized by a Liquid–Crystal Template Mechanism. *Nature* **1992**, *359*, 710–712.
- (13) Zhao, D. Y.; Feng, J. L.; Huo, Q. S.; Meolsh, N.; Fredrickson, G. H.; Chmelka, B. F.; Stucky, G. D. Triblock Copolymer Syntheses of Mesoporous Silica with Periodic 50 to 300 Angstrom Pores. *Science* **1998**, *279*, 548–552.
- (14) Lopez-Orozco, S.; Inayat, A.; Schwab, A.; Selvam, T.; Schwieger, W. Zeolitic Materials with Hierarchical Porous Structures. *Adv. Mater.* **2011**, *23*, 2602–2615.
- (15) Groen, J. C.; Moulinjin, J. A.; Pérez-Ramírez, J. Desilication: On the Controlled Generation of Mesoporosity in MFI Zeolites. *J. Mater. Chem.* **2006**, *16*, 2121–2131.
- (16) Verboekend, D.; Caicedo-Realpe, R.; Bonilla, A.; Santiago, M.; Pérez-Ramírez, J. Properties and Functions of Hierarchical Ferrierite Zeolites Obtained by Sequential Post-synthesis Treatments. *Chem. Mater.* **2010**, *22*, 4679–4689.
- (17) Jacobsen, C. J. H.; Madsen, C.; Houzicka, J.; Schmidt, I.; Carlsson, A. Mesoporous Zeolite Single Crystals. *J. Am. Chem. Soc.* **2000**, *122*, 7116–7117.
- (18) Schmidt, I.; Boisen, A.; Gustavsson, E.; Stahl, K.; Pehrson, S.; Danl, S.; Carlsson, A.; Jacobsen, C. J. H. Carbon Nanotube Templatized Growth of Mesoporous Zeolite Single Crystals. *Chem. Mater.* **2001**, *13*, 4416–4418.
- (19) Zhu, H. B.; Liu, Z. C.; Wang, Y. D.; Kong, D. J.; Yuan, X. H.; Xie, Z. K. Nanosized  $\text{CaCO}_3$  as Hard Template for Creation of Intracrystal Pores within Silicalite-1 Crystal. *Chem. Mater.* **2008**, *20*, 1134–1139.
- (20) Choi, M.; Cho, H. S.; Srivastava, R.; Venkatesan, C.; Choi, D.-H.; Ryoo, R. Amphiphilic Organosilane-Directed Synthesis of Crystalline Zeolite with Tunable Mesoporosity. *Nat. Mater.* **2006**, *5*, 718–723.
- (21) Na, K.; Jo, C.; Kim, J.; Cho, K.; Jung, J.; Seo, Y.; Messinger, R. J.; Chmelka, B. F.; Ryoo, R. Directing Zeolite Structures into Hierarchically Nanoporous Architectures. *Science* **2011**, *333*, 328–332.
- (22) Wang, H.; Pinnavaia, T. J. MFI Zeolite with Small and Uniform Intracrystal Mesopores. *Angew. Chem., Int. Ed.* **2006**, *45*, 7603–7606.
- (23) Xiao, F. S.; Wang, L. F.; Yin, C. Y.; Lin, K. F.; Di, Y.; Li, J. X.; Xu, R.; Su, D. S.; Schlägl, R.; Yokoi, T.; Tatsumi, T. Catalytic Properties of Hierarchical Mesoporous Zeolites Templatized with a Mixture of Small Organic Ammonium Salts and Mesoscale Cationic Polymers. *Angew. Chem., Int. Ed.* **2006**, *45*, 3090–3093.
- (24) Liu, F. J.; Willhammar, T.; Wang, L.; Zhu, L. F.; Sun, Q.; Meng, X. J.; Carrillo-Cabrera, W.; Zou, X. D.; Xiao, F. S. ZSM-5 Zeolite Single Crystals with b-Axis-Aligned Mesoporous Channels as an Efficient Catalyst for Conversion of Bulky Organic Molecules. *J. Am. Chem. Soc.* **2012**, *134*, 4557–4560.
- (25) Zhou, J. A.; Hua, Z. L.; Liu, Z. C.; Wu, W.; Zhu, Y.; Shi, J. L. Direct Synthetic Strategy of Mesoporous ZSM-5 Zeolites by Using Conventional Block Copolymer Templates and the Improved Catalytic Properties. *ACS Catal.* **2011**, *1*, 287–291.
- (26) Van Koningsveld, H.; Jansen, J. C.; van Beckum, H. The Monoclinic Framework Structure of Zeolite H-ZSM-5. Comparison with the Orthorhombic Framework of As-Synthesized ZSM-5. *Zeolites* **1990**, *10*, 235–242.
- (27) Koekkoek, A. J. J.; Tempelman, C. H. L.; Degirmenci, V.; Guo, M. L.; Feng, Z. C.; Li, C.; Hensen, E. J. M. Hierarchical Zeolites Prepared by Organosilane Templating: A Study of the Synthesis Mechanism and Catalytic Activity. *Catal. Today* **2011**, *168*, 96–111.
- (28) Serrano, D. P.; Aguado, J.; Escola, J. M.; Rodriguez, J. M.; Peral, A. Effect of the Organic Moiety Nature on the Synthesis of Hierarchical ZSM-5 from Silanized Protozeolitic Units. *J. Mater. Chem.* **2008**, *18*, 4210–4218.
- (29) Serrano, D. P.; Aguado, J.; Escola, J. M.; Rodríguez, J. M.; Peral, Á. Hierarchical Zeolites with Enhanced Textural and Catalytic Properties Synthesized from Organofunctionalized Seeds. *Chem. Mater.* **2006**, *18*, 2462–2464.
- (30) Li, W. C.; Lu, A. H.; Palkovits, R.; Schmidt, W.; Spliethoff, B.; Schüth, F. Hierarchically Structured Monolithic Silicalite-1 Consisting of Crystallized Nanoparticles and Its Performance in the Beckmann Rearrangement of Cyclohexanone Oxime. *J. Am. Chem. Soc.* **2005**, *127*, 12595–12600.
- (31) Mironov, A. V.; Starodoubtsev, S. G.; Khokhlov, A. R. Effect of Chemical Nature of 1,1-Salt on Structure of Polyelectrolyte Gel–Surfactant Complexes. *J. Phys. Chem. B* **2001**, *105*, 5612–5617.
- (32) Pi, Y. Y.; Shang, Y. Z.; Liu, H. L.; Hu, Y.; Jiang, J. W. Salt Effect on the Interactions between Gemini Surfactant and Oppositely Charged Polyelectrolyte in Aqueous Solution. *J. Colloid Interface Sci.* **2007**, *306*, 405–410.
- (33) Pojjak, K.; Bertalanitis, E.; Meszaros, R. Effect of Salt on the Equilibrium and Nonequilibrium Features of Polyelectrolyte/Surfactant Association. *Langmuir* **2011**, *27*, 9139–9147.